

Impact of Ligand Protonation on Eigen-Type Metal Complexation Kinetics in Aqueous Systems

Herman P. van Leeuwen,^{*,†} Raewyn M. Town,[‡] and Jacques Buffle[§]

Laboratory of Physical Chemistry and Colloid Science, Wageningen University, Dreijenplein 6, 6703 HB Wageningen, The Netherlands, Institute of Physics and Chemistry, University of Southern Denmark, Campusvej 55, DK-5230 Odense, Denmark, and CABE, Section de Chimie – Sciences II, University of Geneva, Quai Ernest-Ansermet 30, CH-1211 Geneva 4, Switzerland

Received: November 6, 2006; In Final Form: January 9, 2007

The impact of ligand protonation on metal speciation dynamics is quantitatively described. Starting from the usual situation for metal complex formation reactions in aqueous systems, i.e., exchange of water for the ligand in the inner coordination sphere as the rate-determining step (Eigen mechanism), expressions are derived for the lability of metal complexes with protonated and unprotonated ligand species being involved in formation of the precursor outer-sphere complex. A differentiated approach is developed whereby the contributions from all outer-sphere complexes are included in the rate of complex formation, to an extent weighted by their respective stabilities. The stability of the ion pair type outer-sphere complex is given particular attention, especially for the case of multidentate ligands containing several charged sites. It turns out that in such cases, the effective ligand charge can be considerably different from the formal charge. The lability of Cd(II) complexes with 1,2-diaminoethane-*N,N'*-diethanoic acid at a microelectrode is reasonably well predicted by the new approach.

1. Introduction

Rigorous understanding of metal speciation in environmental and biological systems is involved, due to the wide ranges of stabilities, labilities, and mobilities of the various complex species.¹ For simple ligands, the role of ligand protonation in determining metal complexation equilibria is well-known: conditional stability constants, K_{cond} , are often used to account for the degree of ligand protonation in the effective binding strength at a given pH. For dynamic features of metal complexes, speciation analysis must go beyond equilibrium considerations. Therefore, increasing effort is needed in study of dynamic metal ion speciation as derived from the kinetic characteristics of interconversion of metal complex species under a variety of conditions. This knowledge is required for establishing sound and predictive relationships between metal ion speciation and bioavailability,² and for interpretation of data furnished by emerging dynamic analytical techniques.^{3,4} A rigorous approach to establishing a dynamic interpretation framework requires consideration of the effective time scale of the processes involved and the rate parameters for the association/dissociation reactions of the complex system of interest.

Many complex formation reactions in aqueous solutions follow the Eigen mechanism, i.e., rapid formation of an outer-sphere complex between the hydrated metal ion, M, and the ligand, L, followed by a slow, rate-limiting dehydration step. The rate of complexation, k_a , is thus generally determined by (i) the rate constant for water substitution in the inner coordination sphere of the metal ion, k_w ,⁵ together with (ii) the stability constant for the intermediate outer-sphere complex, K^{os} . The latter is estimated on the basis of metal–ligand ion pair

electrostatics^{6–8} and is dependent on the charges, z_+ and z_- . For instance, a change of 2 in the product of the charges on the ions, z_+z_- , as may occur on protonation/deprotonation of L, results in a factor of 20 change in K^{os} , and consequently in k_a . Indeed, it has been observed experimentally that for the protonated outer-sphere complex the rate of complex formation is 20–100 times slower than with the stronger unprotonated one.^{9–12} Thus protonation of L generally has a substantial impact on the rate of ML formation. We note, however, that in aqueous solution, ligand protonation reactions themselves are very fast, so various protonated/unprotonated forms are in equilibrium and their interconversion rates do not influence the metal complex formation rate.⁶ It is their equilibrium concentrations that will be relevant for complex formation/dissociation kinetics. Herein we extend current dynamic theory on the lability of metal complexes to account for the protolytic nature of the ligand species involved and their relative contributions to formation/dissociation rate-limiting steps. We follow Eigen mechanism principles and, in this first detailed treatment of the topic, consider formation of 1:1 ML inner-sphere complexes only. More specifically we shall analyze the impact of the charge distribution (different charged sites, either protonated or not) within the ligand entity on the stability of the outer-sphere composite ion pair. We consider in particular the case of a composite, e.g., multidentate, ligand containing several charged sites (not necessarily of equal charge) in different positions, not all of which are involved in the outer-sphere interaction with M. We illustrate the concepts by measurement of the electrochemical lability of Cd(II) complexes with 1,2-diaminoethane-*N,N'*-diethanoic acid (EDDA) at a microelectrode. Needless to add that the principles laid out in this paper are applicable to any dynamic technique for speciation analysis, or (bio)interfacial process, in which one of the metal species is involved.

[†] Wageningen University.

[‡] University of Southern Denmark.

[§] University of Geneva.

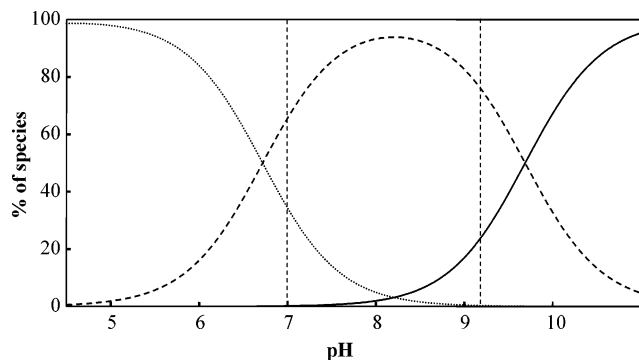


Figure 1. Protonation of EDDA as a function of pH. Vertical dashed lines denote the pH range (7.0–9.2) studied for Cd(II) complexation. Ligand species shown are L^{2-} (solid curve), HL^{-} (dashed curve), and H_2L (dotted curve); amounts of H_3L^{+} and H_4L^{2+} are negligible over the pH range shown. Calculated for $\log \beta_{1H} = 9.69$, $\log \beta_{2H} = 16.41$, $\log \beta_{3H} = 18.78$, and $\log \beta_{4H} = 20.44$.¹⁵

2. Experimental Section

2.1. Apparatus. An Ecochemie μ Autolab potentiostat was used in conjunction with a Metrohm 663 VA stand. The electrometer input impedance of this instrument is > 100 G Ω . The working electrode was a mercury-coated iridium micro-electrode (prepared according to reported protocols);^{13,14} radius of hemispherical droplet *ca.* 6×10^{-6} m). The auxiliary electrode was glassy carbon, and the reference electrode was Ag|AgCl|KCl(sat) encased in a 0.1 mol dm⁻³ KNO₃ jacket. Measurements were performed at 20 °C. SCP measurements were performed with a stripping current of 5×10^{-11} A.

2.2. Reagents. All solutions were prepared with distilled, deionized water from an Elgastat Maxima system (resistivity > 18 M Ω cm). Cd(II) solutions were prepared by dilution of a commercial certified standard from Aldrich. KNO₃ solutions were prepared from solid KNO₃ (BDH, AnalaR). 1,2-Diaminoethane-*N,N'*-diethanoic acid (EDDA) was from Fluka (purity, $> 98\%$). Solutions were initially purged with oxygen-free nitrogen (< 0.1 ppm), then a nitrogen blanket was maintained during measurements.

2.3. Selection of Test Complex. It is not straightforward to find a practical test system that unambiguously illustrates the concepts presented herein. Ideally, we want a ligand with a well-defined spatial distribution of point charges (section 3.3). Furthermore, the lability of the metal complex must be sufficiently low with respect to the kinetic window of the analytical technique employed to be able to measure kinetically controlled responses.⁴ To facilitate data interpretation, it is necessary to have one complex stoichiometry as the predominant solution species over a wide ligand concentration range. Relatively simple ligands, including many inorganic ones, form complexes that are often too labile to be suitable test systems and besides they typically form ML_n species. For our purposes, multidentate ligands, e.g., EDDA, form complexes of appropriate stability and lability, albeit with the drawback that ion pair electrostatics in the outer-sphere intermediate is no longer trivial (section 3.3).

1,2-Diaminoethane-*N,N'*-diethanoic acid (EDDA) (HOOC·CH₂·NH·CH₂·CH₂·NH·CH₂·COOH) has four protonatable functional groups with constants $\log \beta_{1H} = 9.69$, $\log \beta_{2H} = 16.41$, $\log \beta_{3H} = 18.78$, and $\log \beta_{4H} = 20.44$;¹⁵ the speciation distribution of ligand species as a function of pH is given in Figure 1.

Complexation studies were conducted at pH values centered around 8. In this region the concentration of HL^{-} is relatively high and approximately constant, and that of L^{2-} is changing significantly, thus facilitating the distinction between their

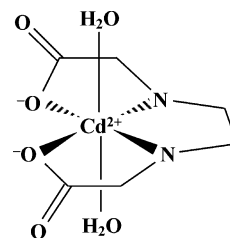


Figure 2. Schematic representation of the inner-sphere CdEDDA complex, with involvement of L^{2-} . In the case involving HL^{-} , one of the two nitrogens is protonated.

respective roles in the Cd(II) complexation kinetics. Because there is some spread in published values for the stability of CdEDDA ($\log K_1$ ranges from 8.6¹⁶ to 10.8¹⁷), we determined the $\log K$ value under our experimental conditions via the shift in SSCP half-wave deposition potential upon complexation.¹⁸ $\log K_{CdEDDA}$ was found to be 8.2 ± 0.1 , and this value was used in the computations. Under our range of experimental conditions the inner-sphere complex ML is the predominant species in solution ($> 80\%$). No evidence has been reported for formation of CdHL inner-sphere complexes with EDDA, not even at pH values as low as 4.5.¹⁹ EDDA-type ligands typically occupy four of the octahedral sites around the metal ion in the *inner-sphere* complex (Figure 2) and form stable complexes with a range of metal ions.^{19,20} See ref 21 for a general review of their complexation properties.

3. Theory

We seek to elucidate the quantitative significance of ligand protonation in metal speciation dynamics, in particular as compared to the operational lability of the complex system for the conventional situation with only the free ligand, L, involved. The application of a lability index, \mathcal{L} , for interpretation of analytical speciation measurements and biouptake has been described in detail elsewhere.⁴ In brief, for a volume reaction, maintenance of equilibrium derives from the pertaining reaction rate constants and the relevant time scale. For the simplest case of a metal ion M forming complexes with ligand L, no matter what intricacies are hidden in the detailed reaction scheme, we write



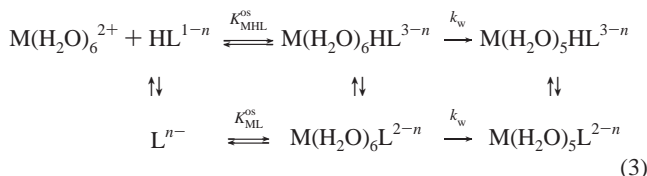
where k_a and k_d are the rate constants for complex association and dissociation, respectively, and k_a/k_d equals the stability constant, K . Under conditions of sufficient excess ligand over metal, the association reaction is quasi-monomolecular with rate constant $k'_a = k_a c_L$. A system that is sufficiently dynamic to maintain volume equilibrium within a time scale, t , obeys the double condition:²²

$$k'_a t, k_d t \gg 1 \quad (2)$$

For the case of an interfacial process in which M is consumed, the overall flux of M toward the interface results from the coupled diffusion and kinetics of interconversion between M and its various species in the complex system. Dynamic metal complex systems are labile if there is frequent interconversion between M and ML during their transport through the diffusion layer; i.e., lability refers to the ability of complexes to maintain equilibrium with the free metal ion, M, within the context of such an ongoing interfacial process.²³

3.1. Protonation of Outer-Sphere Complexes. When protonated ligand species are present, the scheme for the precursor

outer-sphere complex formation becomes more differentiated. For simplicity and clarity, we first tackle the case where only 1:1 inner-sphere ML complexes are formed in a pH range with both L and HL in solution, and both $M(H_2O)_6HL$ and $M(H_2O)_6L$ types of outer-sphere complexes formed. Following the Eigen mechanism principles, and realizing that protonation/deprotonation reactions are fast on time scales where metal ion dehydration takes place, the complete complex formation scheme with two parallel rate-limiting dehydration steps is represented by



The rate constant (k_w) for removal of a water molecule from the complete inner hydration sphere is predominantly determined by the breaking of the metal/oxygen bonds. On the level of the Eigen scheme, it is supposed to be practically unaffected by the presence or absence of the proton in the complexing molecule, L. Hence, we assume that the value of k_w for $M(H_2O)_6HL^{3-n}$ is the same as that for $M(H_2O)_6L^{2-n}$. However, the same is not true for K^{os} : the stability of the outer-sphere complex involving the free ligand L, K_{ML}^{os} , will generally not be the same as that for the protonated ligand, HL, K_{MHL}^{os} . A detailed analysis will be presented in section 3.3. For convenience, from now on the *inner*-sphere complexes are denoted without their remaining inner solvation shell, i.e., MHL and ML, respectively.

The total rate of the (inner-sphere) complex formation, R_a , can thus be written as the sum of the contributions from the two types of outer-sphere complexes, $M(H_2O)_6HL$ and $M(H_2O)_6L$:

$$R_a = k_w c_{M(H_2O)_6HL} + k_w c_{M(H_2O)_6L} = k_w K_{MHL}^{os} c_M c_{HL} + k_w K_{ML}^{os} c_M c_L \quad (4)$$

where c_M is the short-hand notation for $c_{M(H_2O)_6^{2+}}$ and c_{HL} and c_L are the concentrations of protonated and deprotonated L, respectively. Returning to the case of an interfacial process involving consumption of the species M, we have to consider the joint reaction layer²⁴ formed by the two complex species ML and MHL that maintain equilibrium between themselves. According to the Einstein equation, the thickness, μ , of such a reaction layer is determined by the lifetime, τ_M , of free M, formed by dissociation of ML, and its mean diffusional displacement. In the presence of differently protonated forms of the ligand, all these species contribute to μ to an extent weighted by their respective K^{os} values. In the case of L and HL, the overall τ_M is given by

$$\frac{1}{\tau_{M,overall}} = k_{aML} c_L + k_{aMHL} c_{HL} \quad (5)$$

which can be expressed in terms of an effective k'_a value, $k_a^{eff} c_L$, where $k_a^{eff} = k_{aML} + k_{aMHL} \beta_{1H} c_H$.

The reaction layer thickness follows as

$$\mu = \left(\frac{D_M}{k_{aML} c_L + k_{aMHL} c_{HL}} \right)^{1/2} \quad (6)$$

in accordance with the general case of a mixture of complex species.²⁵

With the appropriate expression for the reaction layer thickness at hand, we can formulate the kinetic flux, J_{kin} , of M toward a macroscopic surface as resulting from dissociation of inner-sphere ML complexes:

$$J_{kin} = k_d c_{ML} \mu \quad (7)$$

where c_{ML} is the concentration of inner-sphere complexes, and k_d is the effective overall k_d for the system. For the cases considered in this paper, the presence or absence of H is immaterial for the rate of dissociation, and hence we assume, like we did for water (k_w), that k_d is practically unaffected by protonation of the complexing molecule, L. The proton does of course impact electrostatically, and this is accounted for in K^{os} , as detailed in section 3.3.

The combination of eqs 6 and 7 leads to

$$\log J_{kin} = \log k_d c_{ML} D_M^{1/2} - \frac{1}{2} \log [k_{aML} c_L + k_{aMHL} c_{HL}] \quad (8)$$

Using $\beta_{1H} = c_{HL}/c_H c_L$ and eq 3, this comes to

$$\log J_{kin} = \log k_d c_{ML} D_M^{1/2} - \frac{1}{2} \log [k_w K_{ML}^{os} c_L (1 + \beta_{1H}^{os} c_H)] \quad (9)$$

where

$$\beta_{1H}^{os} = \frac{K_{MHL}^{os}}{K_{ML}^{os}} \beta_{1H} \quad (10)$$

that is, the protonation constant for the outer-sphere acid/base pair MHL^{os}/ML^{os} . The dependence of J_{kin} on pH is thus governed by the distribution of ligand over L and HL, *as well as* by the distribution of their outer-sphere complexes with the metal ion, M.

3.2. Degree of Lability, ξ , and the Lability Index, ζ . The kinetic flux, J_{kin} , is the governing parameter for the so-called lability of a metal complex system. It describes the ability of a dynamic system to maintain equilibrium in the presence of an ongoing interfacial process involving conversion of M. The degree of lability, ξ , expresses the indirect contribution of the complex to the eventual metal flux normalized with respect to its maximum, purely diffusion-controlled, contribution, J_{diff} .^{26,27} For example, for a spherical microelectrode it is given by²⁶

$$\xi = \frac{\kappa_a^{1/2}}{[\epsilon K' (1 + \epsilon K')]^{1/2} + \kappa_a^{1/2}} \quad (11)$$

where $\epsilon = D_{ML}/D_M$, $K' = K_{cL}$, and

$$\kappa_a = \frac{(k_{aML} c_L + k_{aMHL} c_{HL}) r_0^2}{D_M} \quad (12)$$

where r_0 is the radius of the microelectrode. Equation 11 holds for this case because ML and MHL have practically the same D and k_d .

The value of ξ ranges from 0 (nonlabile) to 1 (labile).

For the case of complexes that are sufficiently strong to satisfy $\epsilon K' \gg 1$, i.e., $c_{complex} \gg c_{free\ metal}$, we have

$$\xi \rightarrow \frac{\kappa_a^{1/2}}{\epsilon K' + \kappa_a^{1/2}} \quad (13)$$

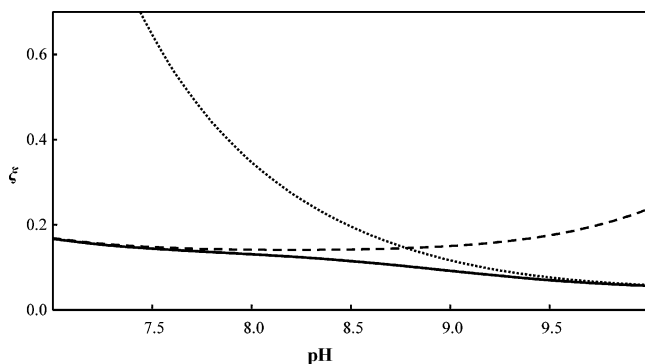


Figure 3. Degree of lability, ξ , as a function of pH for a given k_d with both protonated and deprotonated outer-sphere complexes. The solid curve is ξ computed from the overall kinetic flux (eq 8) that considers both outer-sphere complexes, $M(H_2O)_6L^{2-n}$ and $M(H_2O)_6HL^{3-n}$; the short-dashed curve is that resulting from $M(H_2O)_6L^{2-n}$ only (ξ_L); and the long-dashed curve is from $M(H_2O)_6HL^{3-n}$ only (ξ_{HL}). Parameters used correspond to those applicable to the CdEDDA system: $\log K^{os}(M(H_2O)_6L^{2-n}) = 1.27$, $\log K^{os}(M(H_2O)_6HL^{3-n}) = 0.36$, $k_w = 3 \times 10^8 \text{ s}^{-1}$, $D_M = D_{ML} = 7 \times 10^{-10} \text{ m}^2 \text{ s}^{-1}$, $r_0 = 6 \times 10^{-6} \text{ m}$, $\log K_{ML} = 8.2$, $c_{L,t} = 5 \times 10^{-6} \text{ mol dm}^{-3}$. See text for details.

and then the system achieves lability ($\xi \rightarrow 1$) for

$$\kappa_a^{1/2} \gg \epsilon K' \quad (14)$$

which is identical to the conventional lability criteria (e.g., ref 28) because the degree of lability ξ is related to the well-known lability index, $\mathcal{L}(J_{kin}/J_{dif})$, via $\mathcal{L} = \kappa_a^{1/2}/\epsilon K'$. At the other limit where $\kappa_a^{1/2} \ll \epsilon K'$, ξ is much less than unity and approaches $k_d\mu/(D_{ML}/r_0)$, which again equals the ratio J_{kin}/J_{dif} .

The degree of lability, ξ , computed from the overall kinetic flux, eq 8, is shown in Figure 3, together with that computed from the individual kinetic fluxes that would result if only the deprotonated (ξ_L) or only the protonated (ξ_{HL}) outer-sphere complex is involved in the rate-determining step, i.e., $J_{kin,ML}$ ($=k_d c_{ML}(D_M/k_w K_{ML}^{os} c_L)^{1/2}$), or $J_{kin,MHL}$ ($=k_d c_{MHL}(D_M/k_w K_{MHL}^{os} c_{HL})^{1/2}$), respectively. The computations have been performed for parameters corresponding to the CdEDDA system (see section 3.3). In this case, for $\text{pH} < 9$, c_L is low, and ignoring MHL^{os} in computation of J_{kin} leads to overestimates of the lifetime of free M and the ensuing reaction layer thickness, μ . Similarly, for $\text{pH} > 9$, c_{HL} is low, and ignoring ML^{os} also overestimates the lifetime of free M and μ . The crossover point of the ξ_L and ξ_{HL} curves occurs at $\text{pH} 8.8$ which corresponds to $-\log \beta_{IH}^{os}$ for the conditions considered; eq 10 (see section 3.3).

The relationship between ξ and the experimental measurement is straightforward: the contribution of the complex is obtained by subtracting the term corresponding to the diffusional transport of free metal in the system:²⁷

$$\xi = \frac{X_{ML,kin} - X_{freeM}}{X_{ML,lab} - X_{freeM}} \quad (15)$$

where X is a method-dependent *flux*-related response, e.g., current in voltammetry, τ in SCP, accumulated amount in steady-state diffusive gradients in thin films (DGT), etc. $X_{ML,kin}$ is the analytical signal for the kinetically controlled ML system, X_{freeM} is the signal for the amount of free metal in the ML system, and $X_{ML,lab}$ is the signal for the equivalent labile ML case. The value of X_{freeM} is computed from the pertaining equilibrium constants and that of $X_{ML,lab}$ is taken as the signal for a solution containing metal only, at the same total concentra-

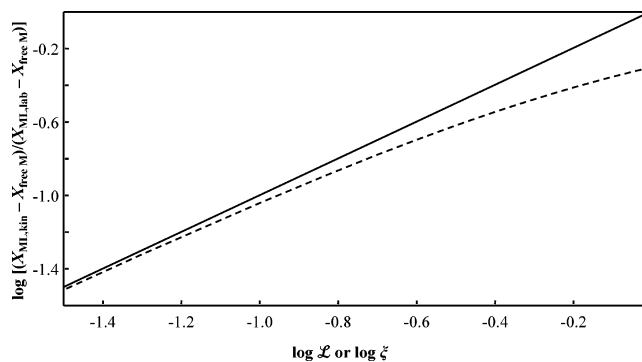


Figure 4. Relationship between the *flux*-type analytical response, X , and the computed degree of lability, ξ (solid line), or the lability index, \mathcal{L} (dashed line). $X_{ML,kin}$ is the analytical signal for the kinetically controlled ML system, $X_{ML,lab}$ is the signal for the equivalent labile ML case, and, X_{freeM} is the signal for the amount of free metal in the ML system.

tion as in the ML system. The relationship between the computed degree of lability ξ , the lability index \mathcal{L} , and the labile fraction measured by a given dynamic technique is shown in Figure 4. Note that the values of ξ and \mathcal{L} approach each other at sufficiently low values, i.e., low c_{freeM} .

3.3. Stability of the Intermediate Outer-Sphere Complex, K^{os} , for Multiply Charged Ligands. According to the Eigen mechanism,²⁹ the rate-limiting step in metal complex formation reactions in aqueous systems is the exchange of water for the ligand in the inner coordination sphere. The relevant precursor is the outer-sphere ion pair of the central metal ion M and the ligand L. The stability of this intermediate outer-sphere complex, K^{os} , is of kinetic importance because it determines the actual concentration of reactive species that undergoes the water exchange in the inner sphere. For a given complex system, the value of K^{os} is usually estimated on the basis of the Fuoss equation,⁸ combined with Debye–Hückel electrostatics for the point charge interaction with inclusion of screening by the surrounding electrolyte solution:³⁰

$$K^{os} = \frac{4\pi}{3} N_{Av} a_g^3 \exp(-U^{os}/kT) \quad (16)$$

with U^{os} representing the interionic potential for a single pair:

$$U^{os} = \frac{z_M z_L e^2}{4\pi\epsilon_0 \epsilon a} \left(1 - \frac{\kappa a}{1 + \kappa a}\right) \quad (17)$$

where z_M is the charge number of the central metal ion, z_L is the charge number of the ligand, $\epsilon_0 \epsilon$ is the permittivity of the electrolyte solution, a is the charge center-to-center distance between M and L, a_g is the geometrical center-to-center distance between M and L, and κ is the reciprocal Debye length of the electrolyte solution, defined by

$$\kappa^2 = e^2 \sum_i z_i^2 c_i N_{Av} / \epsilon_0 \epsilon kT \quad (18)$$

where all symbols have their usual meaning.

The first term between brackets in eq 17 represents the primary Coulombic interaction, and the second one stands for the reduction due to screening by the surrounding electrolyte. For the sake of simplicity, we shall ignore the difference between the geometrical and the charge separations between metal ion and ligand (though this difference is bound to become significant in considering composite ligands, it will not significantly affect our present exercise; see section 3.3.2).

For a composite ligand, L, composed of sites carrying different charges, the interionic potential U^{os} sums all the electrostatic interactions between the central metal ion and the charges on L. Thus the expression for U^{os} as given by eq 17 has to be expanded to

$$U^{\text{os}} = \frac{z_M e^2}{4\pi\epsilon_0\epsilon} \sum_i^n \frac{z_i}{a_i} \left[1 - \frac{\kappa a_i}{1 + \kappa a_i} \right] \quad (19)$$

where z_i is the charge number of site i , n is the total number of charged sites on the ligand L, and a_i the center-to-center distance between i and M. The screening factor $\kappa a_i/(1 + \kappa a_i)$ varies from one site to another with varying a_i . An effective charge number \hat{z}_L for the complete ligand can now be defined by equating the primary Coulombic term $z_M \hat{z}_L e^2/4\pi\epsilon_0\epsilon a$ to the detailed expression (19):

$$\hat{z}_L = a^{\text{os}} \sum_i^n \frac{z_i}{a_i} \left[1 - \frac{\kappa a_i}{1 + \kappa a_i} \right] \quad (20)$$

where a^{os} is the charge center-to-center distance between the primary outer-sphere bound sites and M. For a given ionic strength, the parameter \hat{z}_L expresses the electrostatic effectiveness of a composite ligand L with overall formal charge z_L . It represents all of the Debye–Hückel screening terms, including the primary one in eq 17. In the limit of low ionic strength, where for all i , κa_i approaches zero, \hat{z}_L becomes identical to z_L . By defining \hat{z}_L according to eq 20, one can differentiate between the extent of screening for charged sites i on the ligand at different distances a_i from the coordinating metal ion. For simple ligands, with only one type of charged site and all sites participating in the outer-sphere complex formation, the reference distance a^{os} is identical to a and \hat{z}_L reduces to $z_L[1 - \kappa a/(1 + \kappa a)]$. The intramolecular electrostatic interactions between different charged sites of a certain L count in U^{os} only insofar as they differ between the free L and the outer-sphere complex ML. Such differences may arise if the composite ligand undergoes some reformation to establish a more stable outer-sphere complex that optimally exploits the presence of the different charges. In the next section we shall treat a concrete case to illustrate the impact of the composite nature of the charge of the ligand and the ensuing impact on the effective ligand charge number \hat{z}_L .

3.3.1. Uncertainty in K^{os} . At this stage it is useful to note that the uncertainty involved in the estimation of K^{os} for a composite ligand will be significant. First of all, there are the basic approximations/assumptions in the calculation of the stability of a particular ion pair in an aqueous solution. These include the following:

(i) The ions/charged sites are considered as localized point charges.

(ii) There is no covalent bonding at all between the ion pair partners.

(iii) Apart from the inner hydration sphere of the metal ion, the solvent, water, is considered as a continuous medium; i.e., hydration of the complexing sites is not considered.

(iv) The molar volume of the ion pair is taken as that of a sphere with a radius equal to the charge center-to-center distance between the metal ion and the ligand.

For composite ligands with multiple sites/charges, there are a few *additional* uncertainties in the calculation of ion pair stabilities. We mention here:

(v) The positions of the different charged sites within the ligand molecule, more precisely the distances from their centers to the center of the metal ion, need to be known,

(vi) More often than not, it will be necessary to envisage the possibility of multidentate outer-sphere complexes. These may or may not be realized after reformation of the ligand molecule, which will generally be accompanied by an *increased* internal electrostatic repulsion between the different sites in L,

(vii) It is assumed that interactions between the ligand and water do not change as a result of the ion pair formation and that entropic effects are not significant.

Overall uncertainties in values for K^{os} , as inherent to (i)–(iv), have been estimated as ± 0.2 to ± 0.5 in $\log K^{\text{os}}$ for different metal/ligand combinations.⁴ For the consequences of (v)–(vii) we can use the analysis below for the CdEDDA complex as a guide. Lack of precise information on the various intramolecular site-to-site distances in the ligand molecule typically leads to an error on the order of 10% in the pair energy U^{os} , that is, about ± 0.2 in $\log K^{\text{os}}$ (compare eqs 16 and 17). The calculations for CdEDDA also underscore the importance of considering multidentate outer-sphere complexes. Overlooking this option may give rise to dramatic errors on the level of several units in $\log K^{\text{os}}$. Interestingly enough, such an error is somewhat compensated for by fully counting a remote site in z_L although, in the not too low ionic strength regime, the extent of electrostatic screening by the surrounding electrolyte (see eq 17) disqualifies any estimation on the basis of integer values of z_L . Taken all together, it may be concluded that generally the overall uncertainty in $\log K^{\text{os}}$ is at least on the order of ± 0.5 .

3.3.2. K^{os} for CdEDDA. The structure, dimensions, and proton speciation for EDDA and the inner-sphere CdEDDA complex are given in the Experimental Section. For outer-sphere complex formation with $\text{Cd}(\text{H}_2\text{O})_6^{2+}$, there are two reasonable a priori options, that is, the deprotonated $\text{Cd}(\text{H}_2\text{O})_6\text{L}$ or the protonated $\text{Cd}(\text{H}_2\text{O})_6\text{HL}^+$.

3.3.2.a. $\text{Cd}(\text{H}_2\text{O})_6\text{L}$. In the case of L^{2-} as the outer-sphere ligand, the position of the two nitrogens in EDDA does not matter because they carry no charge. The most favorable ion pair is then obtained with both carboxylates in the outer sphere of M. Taking the diameter of the $\text{Cd}(\text{H}_2\text{O})_6^{2+}$ ion as approximately 0.45 nm,³¹ and positioning of the two (carboxylate) oxygens in trans configuration, the carboxylate–carboxylate distance would be between 0.6 and 0.7 nm. Because in the free L^{2-} , the carboxylate–carboxylate distance is about 1 nm (estimated from the number of single bonds, each of length ca. 0.15 nm),³² there is a small repulsive contribution in the M|L ion pair interaction. If we now compute U^{os} on the basis of eq 19 for a 0.1 mol dm^{-3} electrolyte solution with a Debye length (κ^{-1}) of 1 nm and the dimensions given above, we find that the primary electrostatic interaction between the central Cd^{2+} and the two carboxylates is reduced by some 30% due to screening. Equivalently we can say that the effective charge number \hat{z}_L is -1.4 (cf. the formal z_L of -2). The increased carboxylate–carboxylate repulsion can be accounted for by adding the change in repulsion (as compared to free L) to U^{os} , which for the present case leads to a further reduction by 3%. In passing, we note that the trans conformation is the optimum one because moving one of the carboxylates away from the Cd^{2+} has a stronger impact on the attraction term than on the repulsion. Using eq 16, the overall result may also be given in terms of the outer-sphere complex stability K^{os} for $\text{Cd}(\text{H}_2\text{O})_6\text{EDDA}^{2+}$, which in a 0.1 mol dm^{-3} 1:1 electrolyte comes to $\log K^{\text{os}} = 1.27$, with $\hat{z}_L = -1.33$.

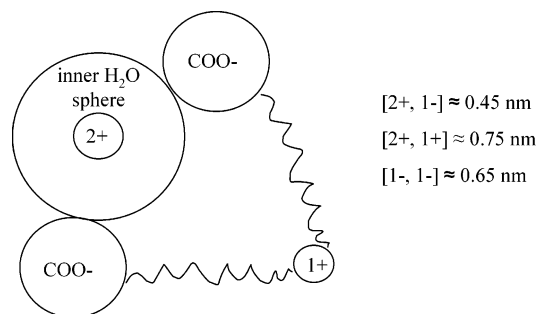


Figure 5. Approximate configuration of the outer-sphere complex of Cd^{2+} with EDDA, $\text{Cd}(\text{H}_2\text{O})_6\text{HL}^+$.

3.3.2.b. $\text{Cd}(\text{H}_2\text{O})_6\text{HL}^+$. At pH 8, the dominant species of EDDA carries one proton at one of the amine groups; i.e., there are two negative carboxylates and one positive NH^+ group. The most favorable conformation of EDDA in an ion pair with Cd^{2+} will then be with the two COO^- in the outer-sphere and the NH^+ at larger distance. Taking into account the various dimensions given above, we may estimate an approximate geometry as sketched in Figure 5. Applying the proposed approach means counting an additional Cd^{2+} – NH^+ repulsion term as compared to the analysis for $\text{Cd}(\text{H}_2\text{O})_6\text{L}$ above. For the same conditions, this leads to a further reduction of U^{os} by almost 28%. The resulting $\log K^{\text{os}}$ is 0.36. The \hat{z}_L now comes to -0.76 , i.e., substantially less negative than the -1.33 for the deprotonated $\text{Cd}(\text{H}_2\text{O})_6\text{L}$ and the formal -1 of HL^- itself.

The difference between the K^{os} values for $\text{Cd}(\text{H}_2\text{O})_6\text{HL}^+$ and $\text{Cd}(\text{H}_2\text{O})_6\text{L}$ can be used to estimate the acid–base constant of the former acid. According to the above results, the ΔU^{os} between the two is 8.5×10^{-20} J, which corresponds to a $\Delta \log \beta_{1\text{H}}$ of about 0.9 (the deprotonated form is favored over the protonated one). Thus the ratio $c_{\text{Cd}(\text{H}_2\text{O})_6\text{L}}/c_{\text{Cd}(\text{H}_2\text{O})_6\text{HL}^+}$ is by a factor of approximately 8 higher than the ratio $c_{\text{L}^{2-}}/c_{\text{HL}^-}$, which is reflected in the $\beta_{1\text{H}}^{\text{os}}$ value of $10^{8.6}$ cf. $\beta_{1\text{H}}$ of $10^{9.7}$ (eq 10). This result is of additional importance for the metal complexation kinetics because it modifies the concentrations of the reactive species $\text{Cd}(\text{H}_2\text{O})_6\text{L}$ and $\text{Cd}(\text{H}_2\text{O})_6\text{HL}^+$.

4. Results and Discussion

The applicability of the theory presented above is tested by comparing the computed kinetic features to the measured microelectrode lability of Cd(II) complexes with EDDA as a function of pH. Until now, tests of lability concepts have largely been concerned with identifying a consistent trend with kinetic window⁴ or obtaining agreement with a predicted dependence on ligand concentration in the case of ML_n complexes.³³ Here the main objective is to distinguish between kinetic interpretations with and without invoking the impact of ligand protonation.

The dynamic features of cadmium 1:1 complexes with the multidentate ligand 1,2-diaminoethane-*N,N'*-diethanoic acid (EDDA) fall within a useful kinetic window to illustrate the concepts presented above. Microelectrode measurements of Cd(II) in the absence and presence of EDDA were made in the pH range 7.0–9.2. This pH range is most suitable for our present purposes because it facilitates distinction of the respective roles of HL^- and L^{2-} in the kinetics. At lower pH, H_2L would also have to be considered in the differentiated scheme (eq 3) and the likelihood of MHL inner-sphere complexes will have to be envisaged, whereas at higher pH, Cd(II) hydrolysis becomes important. For the ligand concentrations used herein, inner-sphere ML complexes are the predominant species over the pH range studied (see section 2.3), and Cd(II) hydrolysis is

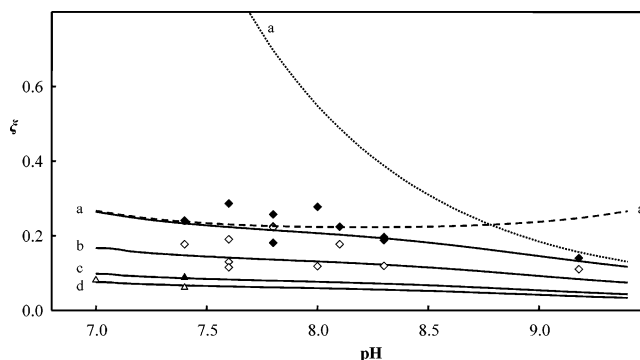


Figure 6. Comparison of the measured and computed degree of lability of CdEDDA complexes as a function of pH. Calculated curves are shown for (i) the overall kinetic flux as resulting from the outer-sphere precursor complexes $\text{M}(\text{H}_2\text{O})_6\text{L}^{2-n}$ and $\text{M}(\text{H}_2\text{O})_6\text{HL}^{3-n}$ (cf. eq 3), solid curves a–d; (ii) that resulting from outer-sphere complex $\text{M}(\text{H}_2\text{O})_6\text{L}^{2-n}$ only, short-dashed curve a; and (iii) that resulting from outer-sphere complex $\text{M}(\text{H}_2\text{O})_6\text{HL}^{3-n}$ only, long-dashed curve a, for total ligand concentrations (a) 2×10^{-6} , (b) 5×10^{-6} , (c) 1.45×10^{-5} , and (d) 2.40×10^{-5} mol dm^{-3} . Parameters used: $\log K^{\text{os}}(\text{M}(\text{H}_2\text{O})_6\text{L}^{2-n}) = 1.27$, $\log K^{\text{os}}(\text{M}(\text{H}_2\text{O})_6\text{HL}^{3-n}) = 0.36$, $k_w = 3 \times 10^8 \text{ s}^{-1}$, $D_M = D_{\text{ML}} = 7 \times 10^{-10} \text{ m}^2 \text{ s}^{-1}$,³⁴ $r_0 = 6 \times 10^{-6} \text{ m}$, $\log K_{\text{ML}} = 8.2$. Experimental data are shown for total ligand concentrations of (\blacklozenge) 2×10^{-6} , (\diamond) 5×10^{-6} , (\blacktriangle) 1.45×10^{-5} , and (\triangle) 2.40×10^{-5} mol dm^{-3} .

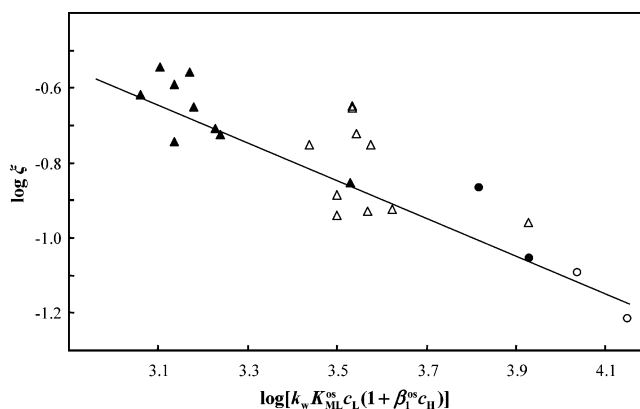


Figure 7. Plot of $\log \xi$ vs $\log [k_w K_{\text{ML}}^{\text{os}} c_{\text{L}} (1 + \beta_{1\text{H}}^{\text{os}} c_{\text{H}})]$, eq 9. The calculated solid line has the theoretical slope of -0.5 and is independent of the total ligand concentration. See Figure 6 caption for values of parameters used. Experimental data are shown for total ligand concentrations of (\blacktriangle) 2×10^{-6} , (\triangle) 5×10^{-6} , (\bullet) 1.45×10^{-5} , and (\circ) 2.40×10^{-5} mol dm^{-3} .

negligible ($*K_1(\text{Cd}(\text{H}_2\text{O})_6^{2+} \rightleftharpoons \text{Cd}(\text{H}_2\text{O})_5\text{OH}^+ + \text{H}^+) = 10^{-10}$ mol dm^{-3}).¹⁵ In all cases there is excess total ligand over total metal in our systems, and the buffering of the concentrations of the relevant ligand species, i.e., L^{2-} and HL^- , is fast. As outlined in section 3.2, the predicted degree of lability, ξ , eq 11, is computed by summing the contributions of the protonated and deprotonated outer-sphere complexes to the kinetic flux, eq 9. These are weighted by their respective stabilities ($\log K_{\text{ML}}^{\text{os}} = 1.27$, $\log K_{\text{MHL}}^{\text{os}} = 0.36$; section 3.3), together with the value of K_{ML} for which we found $10^{8.2} \text{ dm}^3 \text{ mol}^{-1}$ (section 2.3) and the average reported k_w for Cd(II) ($3 \times 10^8 \text{ s}^{-1}$).⁶ The experimental value of ξ is determined by application of eq 15. Figures 6 and 7 clearly show that only the multi outer-sphere approach provides a good description of the experimental data. For a range of ligand concentrations, the experimentally measured degree of lability follows the trend prescribed by the combined impact of both the unprotonated and the protonated outer-sphere complexes. The curve calculated for the unprotonated ligand only, much more strongly increases with decreasing pH than the experimental one. Ignoring the outer-sphere

complex of the protonated ligand HL apparently leads to gross overestimation of τ_M (cf. eq 5) and correspondingly in overestimated values for the reaction layer thickness μ and the kinetic current J_{kin} . The logarithmic representation shown in Figure 7 illustrates that the theoretical framework presented here is an appropriate descriptor of the experimental data (cf. eq 9: for small ξ , it is proportional to J_{kin}). The limiting situations provide further support; i.e., at a relatively low pH of 7 the contribution from $M(H_2O)_6HL^{3-n}$ dominates and converges with the overall value, whereas in the range of pH above 9, the contribution from $M(H_2O)_6L^{2-n}$ dominates the overall ξ . Considering the uncertainties involved, the agreement between the theoretical and experimentally measured values of ξ also provides convincing support for the values of K^{os} and K_{ML} that were determined by independent means (see sections 3.3.2 and 2.3, respectively).

5. Conclusions

On the basis of the Eigen mechanism for complex formation in aqueous systems, we have determined the impact of ligand protonation on metal complexation kinetics. The treatment involves a differentiated approach which considers the simultaneous effects of both unprotonated and protonated outer-sphere complexes on the kinetic flux, weighted by their respective stabilities, K^{os} . For composite ligands with sites of different charge, the computation of the electrostatically defined value for K^{os} is elaborated. The nature and magnitude of the uncertainties involved in this computation are highlighted. The combined kinetic flux is included in the expression for the degree of lability, ξ , of the metal complex system, and compared with the measured lability of CdEDDA complexes as a function of pH at a microelectrode. Within the confines of the uncertainties of the various parameters involved, the computed and measured labilities are in convincing agreement. The results show that the conventional approach, with consideration of the free ligand L only, increasingly overestimates the lability of the system with decreasing pH in the range where the protonated outer-sphere complex is significant. This first detailed treatment of the topic, in which we consider formation of 1:1 ML inner-sphere complexes only, lays the foundations for extension to more involved systems, for example if MHL inner-sphere complexes are present, and/or if more complex mechanisms come into play, e.g., if loss of a second water molecule becomes rate determining, as reported for EDTA.³⁴ The analysis presented herein is generally applicable for understanding the impact of ligand protonation on metal complexation kinetics in the presence of any interfacial process involving consumption of M (or any other species), e.g., biouptake.

Symbols and Abbreviations

- α = degree of protonation of the ligand = $c_L/(c_L + c_{HL})$
 c_M = concentration of free metal (mol dm⁻³)
 $c_{M,t}$ = concentration of total metal (mol dm⁻³)
 c_L = concentration of free ligand (mol dm⁻³)
 $c_{L,t}$ = concentration of total ligand (mol dm⁻³)
 δ = diffusion layer thickness (m)
 D = diffusion coefficient (m² s⁻¹)
 J = flux (mol m⁻² s⁻¹)
 κ = reciprocal Debye length (m⁻¹)
 K = stability constant (dm³ mol⁻¹)
 k_a = complex formation rate constant (dm³ mol⁻¹ s⁻¹)
 k_d = complex dissociation rate constant (s⁻¹)
 k_w = rate constant for water substitution (s⁻¹)
 ML_{os} = outer-sphere complex
 μ = reaction layer thickness (m)

- \mathcal{L} = lability index (dimensionless)
 ξ = degree of lability (dimensionless)
 r_0 = radius of microelectrode (m)
 U^{os} = interionic potential for an ion pair (J)
 z_L = effective ligand charge

Acknowledgment. This work was performed within the ECODIS project, funded by the European Commission's sixth framework program, subpriority 6.3 "Global Change and Ecosystems", under contract 518043. J.B. also thanks the Swiss National Foundation for support under project no. 200020-101974, and R.M.T. thanks the Danish Statens Naturvidenskabelige Forskningsråd for support under rammebevilling 21-04-0525.

References and Notes

- Buffle, J. *Complexation Reactions in Aquatic Systems. An Analytical Approach*; Ellis Horwood: Chichester, U.K., 1988.
- van Leeuwen, H. P.; Köster, W., Eds. *Kinetics and Transport at Biointerfaces*; Buffle, J., van Leeuwen, H. P., Series Eds.; IUPAC Series on Analytical and Physical Chemistry of Environmental Systems, Vol. 9; Wiley: Chichester, U.K., 2004.
- Buffle, J.; Horvai, G., Eds. *In Situ Monitoring of Aquatic Systems: Chemical Analysis and Speciation*; Buffle, J., van Leeuwen, H. P., Series Eds.; IUPAC Series on Analytical and Physical Chemistry of Environmental Systems, Vol. 6; Wiley: Chichester, U.K., 2000.
- van Leeuwen, H. P.; Town, R. M.; Buffle, J.; Cleven, R. F. M. J.; Davison, W.; Puy, J.; van Riemsdijk, W. H.; Sigg, L. *Environ. Sci. Technol.* **2005**, *39*, 8545.
- Eigen, M. *Pure Appl. Chem.* **1963**, *6*, 97.
- Morel, F. M. M.; Hering, J. G. *Principles and Applications of Aquatic Chemistry*; Wiley: New York, 1993.
- Eigen, M. *Z. Phys. Chem.* **1954**, *1*, 176.
- Fuoss, R. *J. Am. Chem. Soc.* **1958**, *80*, 5059.
- Hubbard, C. D. *Inorg. Chem.* **1971**, *10*, 2340.
- Rabenstein, D. L.; Kula, R. J. *J. Am. Chem. Soc.* **1969**, *91*, 2492.
- Reed, G. H.; Kula, R. J. *Inorg. Chem.* **1971**, *10*, 2050.
- Dominey, L. A.; Kustin, K. *Inorg. Chem.* **1984**, *23*, 103.
- Tercier, M. L.; Parthasarathy, N.; Buffle, J. *Electroanalysis* **1995**, *7*, 55.
- van Leeuwen, H. P.; Town, R. M. *J. Electroanal. Chem.* **2002**, *523*, 16.
- Mini-SCDatabase, Academic Software, U.K.
- Huang, Z. X.; Alfalahi, H. S.; Cole, A.; Duffield, J. R.; Furnival, C.; Jones, D. C.; May, P. M.; Smith, G. L.; Williams, D. R. *Polyhedron* **1982**, *1*, 153.
- Nozaki, T.; Hashimoto, T. *Nippon Kagaku Kaishi* **1973**, 1794.
- van Leeuwen, H. P.; Town, R. M. *J. Electroanal. Chem.* **2002**, *536*, 129.
- Chaberek, S.; Martell, A. E. *J. Am. Chem. Soc.* **1952**, *74*, 6228.
- Degischer, G.; Nancollas, G. H. *Inorg. Chem.* **1970**, *9*, 1259.
- Sabo, T. J.; Grgurić-Sipka, S. R.; Trifunović, S. R. *Synth. React. Inorg. Metal-Org. Chem.* **2002**, *32*, 1661.
- de Jong, H. G.; van Leeuwen, H. P. *J. Electroanal. Chem.* **1987**, *235*, 1.
- van Leeuwen, H. P.; Cleven, R. F. M. J.; Buffle, J. *Pure Appl. Chem.* **1989**, *61*, 255.
- Heyrovský, J.; Kuta, J. *Principles of Polarography*; Academic Press: New York, 1966.
- Salvador, J.; Garcés, J. L.; Galceran, J.; Puy, J. *J. Phys. Chem. B* **2006**, *110*, 13661.
- Galceran, J.; Puy, J.; Salvador, J.; Cecília, J.; van Leeuwen, H. P. *J. Electroanal. Chem.* **2001**, *505*, 85.
- Salvador, J.; Puy, J.; Cecília, J.; Galceran, J. *J. Electroanal. Chem.* **2006**, *588*, 303.
- van Leeuwen, H. P. *Electroanalysis* **2000**, *13*, 826.
- Eigen, M.; Wilkins, R. G. *Adv. Chem. Ser.* **1965**, *49*, 55.
- Lyklema, J. *Fundamentals of Interface and Colloid Science. Vol. 1. Fundamentals*; Academic Press: London, 1991.
- Marcus, Y. *J. Chem. Soc., Faraday Trans.* **1991**, *87*, 2995.
- Lide, D. R., Ed. *Handbook of Chemistry and Physics*, 87th ed.; CRC Press: Boca Raton, FL, 2006.
- van Leeuwen, H. P.; Town, R. M. *J. Electroanal. Chem.* **2006**, *587*, 148.
- Rorabacher, D. B.; Margerum, D. W. *Inorg. Chem.* **1963**, *85*, 297.